UCID- 17825

# Lawrence Livermore Laboratory

THE DESIGN OF A CONTINUOUSLY OPERATED 1-keV DEUTERIUM-ION EXTRACTOR

J. H. Fink*

June 12, 1978

*On loan from Westinghouse Electric Corp.

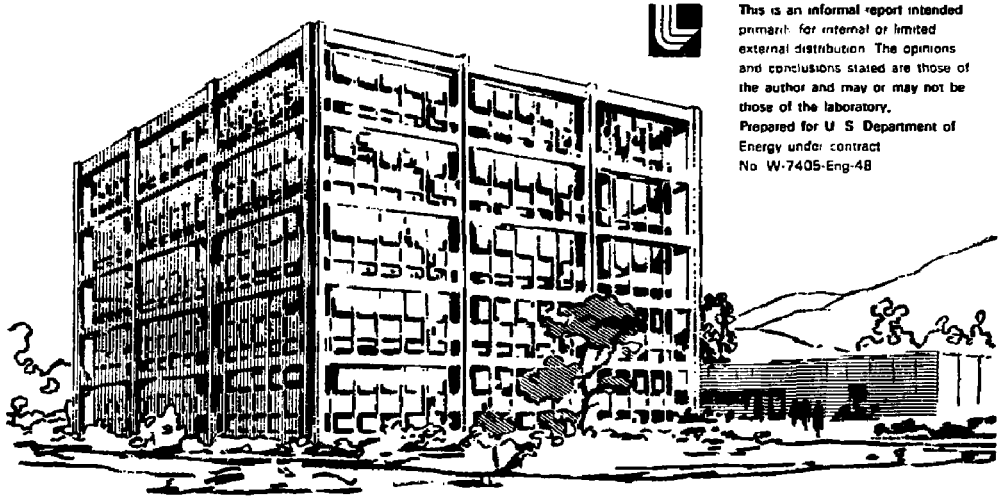

CONTENTS

# THE DESIGN OF A CONTINUOUSLY OPERATED 1-keV DEUTERIUM-ION EXTRACTOR


## ABSTRACT

A novel grid structure that is cooled only by radiation and conduction is shown to be capable of continuously extracting 2.5 $kA \cdot m^{-2}$ of 1-keV positive deuterium ions while dissipating a power loading of 0.4 $MW \cdot m^{-2}$


## INTRODUCTION

In a continuously operated neutral-beam injector, the grid configuration is critical. Shaped to extract ions from the ion source, and spaced to form a beam of desired current density, the grids must be precisely aligned to focus the beam. To sustain high current density, they are subjected to high electric fields as well as to a continuous bombardment of electrons and ions. As a result, the grid contours must be rounded to inhibit voltage breakdown, while the grid design must allow for the dissipation of the energy of the bombarding particles. Finally, to make the system reliable, the grids must be made of a metal, preferably molybdenum or tungsten, that is not prone to arc-over and that will impede sputtering.

Because the performance of the neutral-beam injector is so dependent upon grid reliability, no compromise with quality can be tolerated. As a consequence, the grids must be made with precision regardless of the cost. Fortunately this is not a critical factor, because the grid cost is such a small fraction of the total cost of the injector.

This paper consists of a series of calculations relevant to a particular ion-extractor design. The grids under consideration are part of a positive-ion extractor used in a continuously operated high-energy neutral-beam line. The extractor injects 1-keV deuterium ions into a cesium, double charge-exchange cell, from which 20% of the incident positive ions exit as negatives.

## EXTRACTOR DESIGN

The grids discussed in this paper are of a novel design. Constructed from comb-like sections, they use the comb teeth as grid rods, while the extracted ions flow through the gaps between the teeth. The grid rods, cooled by radiation and conduction, are free to expand. The water-cooled backs of the combs serve as part of the grid frame, holding the rods in place and removing heat.

A diagram of a three-grid, positive-ion extractor is shown in Fig. 1. Each grid is made of two comb sections mounted, open end to open end, with the grid rods overlapping at the center of the grid assembly. The rounded grid contours needed to shape the beam are subsequently formed by electron discharge machining. The three-grid, 1-keV extractor is shown in Fig. 2.

The extractor is assembled by a sequence of brazes, each at a lower temperature than its predecessor. Precise alignment is achieved with carbon jigs that hold the parts in place during the brazes. Grid 1 is fixed to grid 3 with several small, button-like alumina insulators, designed to hold off 1 kV. Meanwhile, grid 2 is fastened to grid 1 via several hollow alumina tubes that hold off 15 kV. These feedthroughs provide access for cooling water as well as for the electrical connection to grid 2. The metal flanges joining the alumina tubes to the grids are designed to act as springs. They protect the alumina by limiting the stress that would result from a thermal mismatch between the grids. Over the 0.4 m of grid length, the mismatch is less than 0.025 mm if the temperatures of the two grid frames are held to within 15°C of each other.

The grid structures are designed to shield the alumina insulators from the ion beam and to form baffles that prevent any cesium vapor, escaping from the charge-exchange cell, from depositing on the insulator surfaces.

## PHYSICAL CONSTRAINTS ON OBTAINABLE ION CURRENT DENSITY

The maximum current density obtained from an ion source is limited by physical constraints imposed by the ion extractor. In the following, we investigate these constraints and establish relationships between the accel voltage, the extracted current density, and the inter-electrode spacings.

A simple, two-grid extractor designed to deliver a beam of current density J at some potential V will have an effective grid spacing of

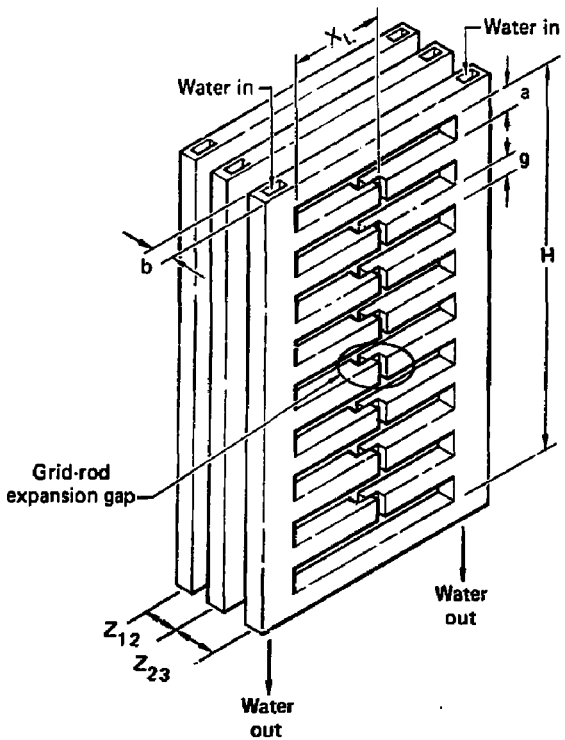


Fig. 1. Configuration of a three-grid, positive-ion extractor.

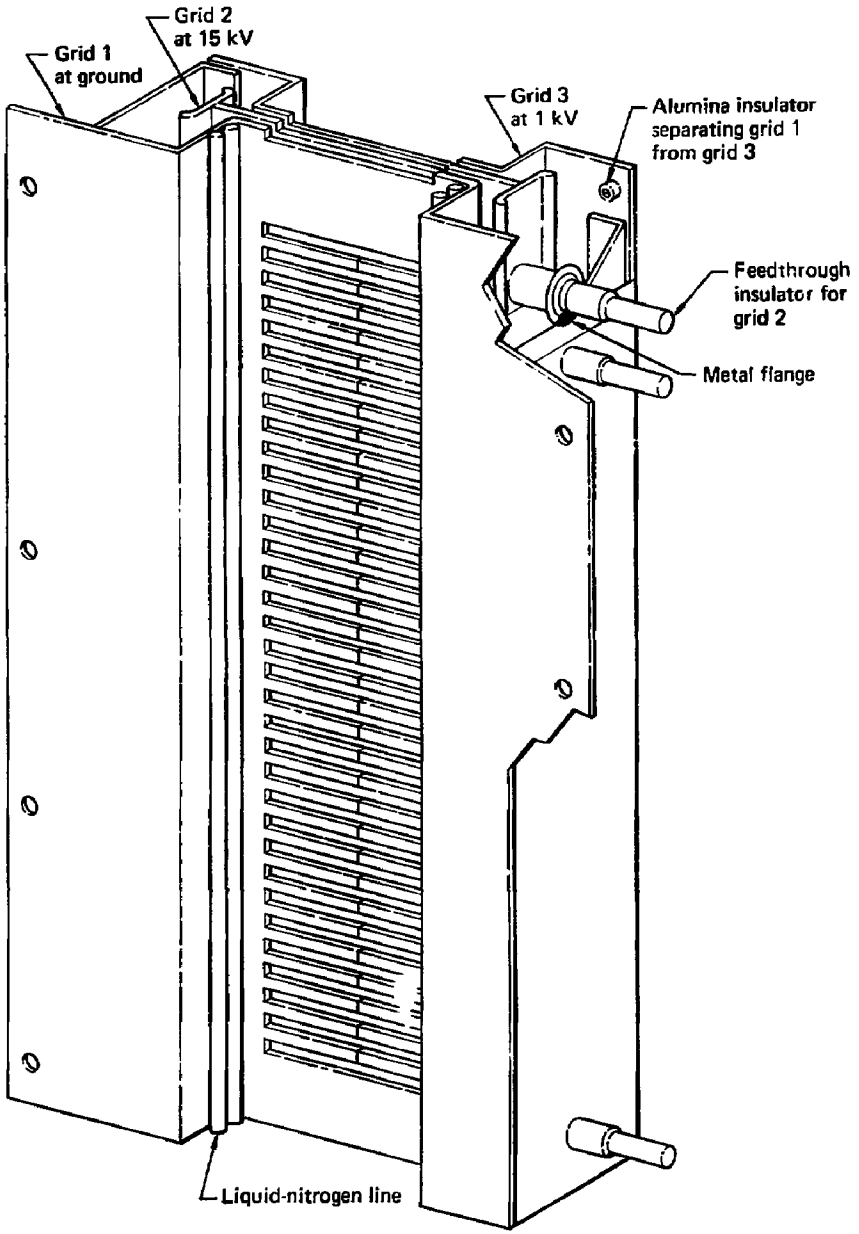


Fig. 2. The three-grid, 1-keV, positive deuterium-ion extractor.

$$z_0 = (q/J)^{1/2} V^{3/4} ,$$

in which q is the perveance of the extractor in accordance with Child's law.

For a planar structure extracting a beam of mixed molecular species, the perveance is

$$q = \frac{4\varepsilon_0}{9} \left(\frac{2e}{M_D}\right)^{1/2} \left(\eta_1 + \sqrt{2}\,\eta_2 + \sqrt{3}\,\eta_3\right) ,$$

where $\varepsilon_0$ is the permittivity of vacuum, e is the charge on an electron, $M_D$ is the mass of a deuterium ion, and $\eta_1$, $\eta_2$, and $\eta_3$ represent the fractions of $D_1$, $D_2$, and $D_3$ ions in the beam. Thus, for typical values of $\eta_1$ = 75%, $\eta_2$ = 15%, and $\eta_3$ = 10%, the perveance is $q = 3.4 \times 10^{-8}$ A•V$^{-3/2}$.

Using the preceding equations, we find that the grid spacing required to deliver a 1-keV beam is a function of the desired current density; i.e.,

$$z_0 = (3.28 \times 10^{-3})\, J^{-1/2} ,$$

for which calculated values are shown in Fig. 3. The resulting inter-electrode spacings are small, making the two-grid extractor impractical because it does not provide sufficient room for thick grids of adequate rigidity Thus, a three-grid configuration is used because it permits larger inter-electrode spacings.

A typical potential profile through a three-grid extractor is shown in Fig. 4. The ions are drawn out of the source by the negative potential $V_2$ on grid 2, to be subsequently decelerated by a potential $V_3$ on grid 3. Figure 5 shows the approximate shapes of the cross sections of the grid rods. The precise grid contours are determined by computer studies of the ion trajectories.

If we assume $V_1 = 0$, the extracted ion current density is

$$J = q \frac{V_2^{3/2}}{z_{12}^2} ,$$

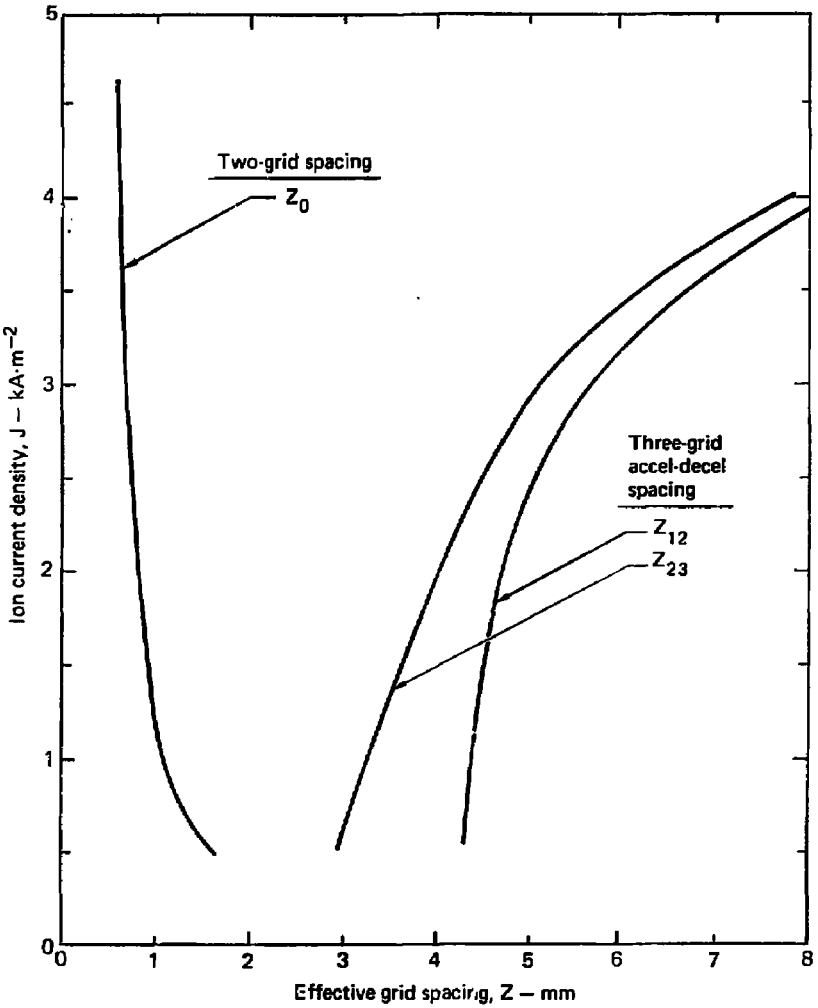


Fig. 3. Comparison between the grid spacings for two- and three-grid extractors of 1-keV deuterium ions, where $Z_{12}$ is the spacing between the centers of grids 1 and 2, etc.

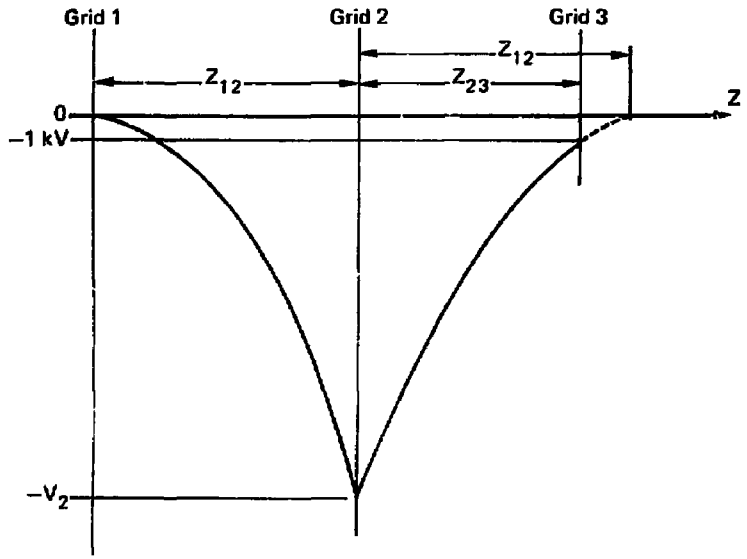


Fig. 4. Potential profile of the accel-decel grids in a three-grid, 1-keV extractor.

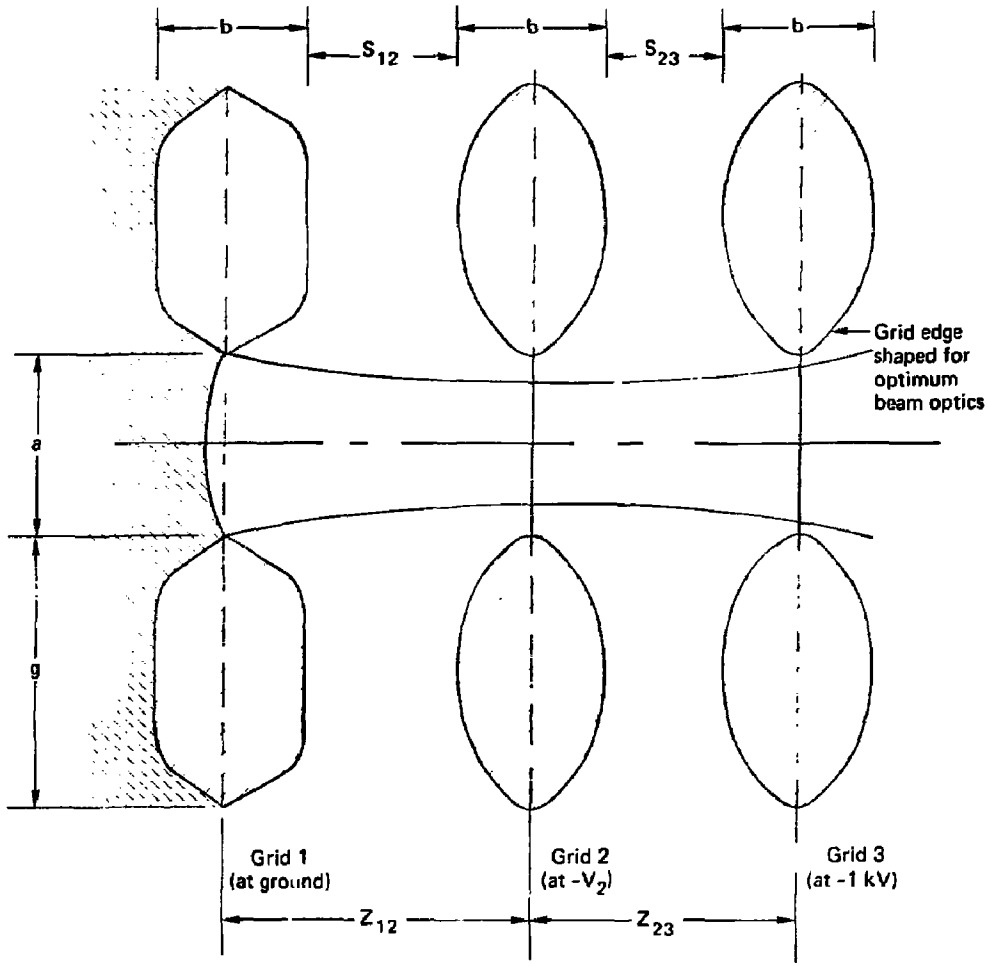


Fig. 5. Cross sections of the grids of a 1-keV extractor.

where $Z_{12}$ is the effective spacing between grid 1 and grid 2. By symmetry, it can be seen that

$$J = q \frac{V_3^{3/2}}{(Z_{12} - Z_{23})^2} ,$$

where $Z_{12}$ is the spacing between grid 2 and an imagined ion source on the grid 3 side of grid 2, and where $Z_{23}$ is the actual spacing between grids 2 and 3.

Because the current density does not vary greatly through the extractor, the preceding equations can be combined to give

$$Z_{12} = \frac{Z_{23}}{1 - (V_3/V_2)^{3/4}} ,$$

and

$$J = q \left[ \frac{V_2^{3/4} - V_3^{3/4}}{Z_{23}} \right]^2 .$$

Calculated relationships between the current density J and $Z_{12}$, $Z_{23}$ are shown in Fig. 3, for $V_3$ = 1 kV. For the same extracted current density, the spacings in the three-grid extractor are considerably larger than those in the two-grid system.

The center-to-center spacing between grid 2 and grid 3, as shown in Fig. 5, can be described by

$$Z_{23} = b + S_{23} ,$$

in which b is the grid thickness and $S_{23}$ is the actual gap between the grids. Thus, if $E_{av}$ is the average electric field strength between adjacent grids,

$$s_{23} = \frac{V_2 - V_3}{E_{av}} ,$$

and

$$J = q\left[\frac{V_2^{3/4} - V_3^{3/4}}{b + (V_2 - V_3)/E_{av}}\right]^2 .$$

As a design parameter, $E_{av}$ is critical. This can be seen in Fig. 6, where b is taken to be 2.5 mm and J is plotted for three different values of $E_{av}$ as a function of the accel voltage $V_2$. If the electric field strength is too low, the extracted ion current density will be less than it need be, requiring a larger ion source to maintain the desired beam current. If the electric field strength is too high, frequent arc-overs result, causing the system reliability to suffer.

The grid thickness b also has a marked effect on the extracted ion current density. This is shown in Fig. 7 for $E_{av}$ = 0.75 MV•m$^{-1}$.

Because the grid power loading is high to accommodate the maximum allowable ion current density, the grids must be water cooled. Thus, the grid thickness b must be adequate to permit water to flow through the grid. To accommodate a water line 1.5 mm wide, the grid thickness b must be at least 2.5 mm.

Values of $z_{12}$ and $z_{23}$ are shown as a function of the accel voltage $V_2$ in Fig. 8 where b is assumed to be 2.5 mm and $E_{av}$ is 0.75 MV•m$^{-1}$.

## GRID POWER LOADING

The anticipated grid power loading is a critical design parameter. In this section, we estimate the power loading on the extractor grids as a function of the accel voltage $V_2$.

We assume that the extractor is constructed with sufficient precision to ensure its interception of only a negligible fraction of the primary beam ions. Grid loading is then a consequence of bombardment by ions formed in the space between the grids.[1] These ions are generated by charge exchange and ionization caused by the passage of the primary beam through the background gas.

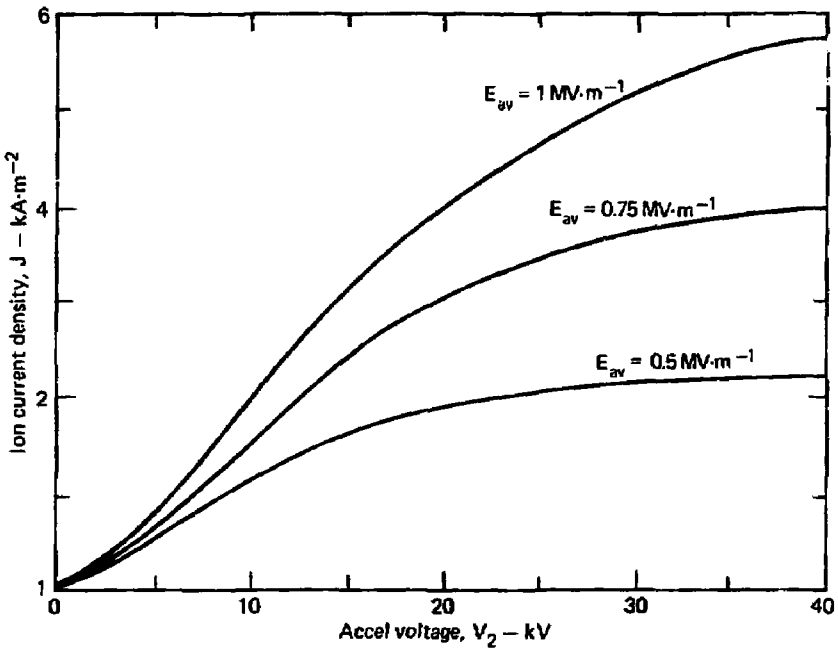


Fig. 6. Extracted ion current density (for 2.5-mm-thick grids) as a function of the accel potential, where $E_{av}$ is the average electric field strength between the grids.

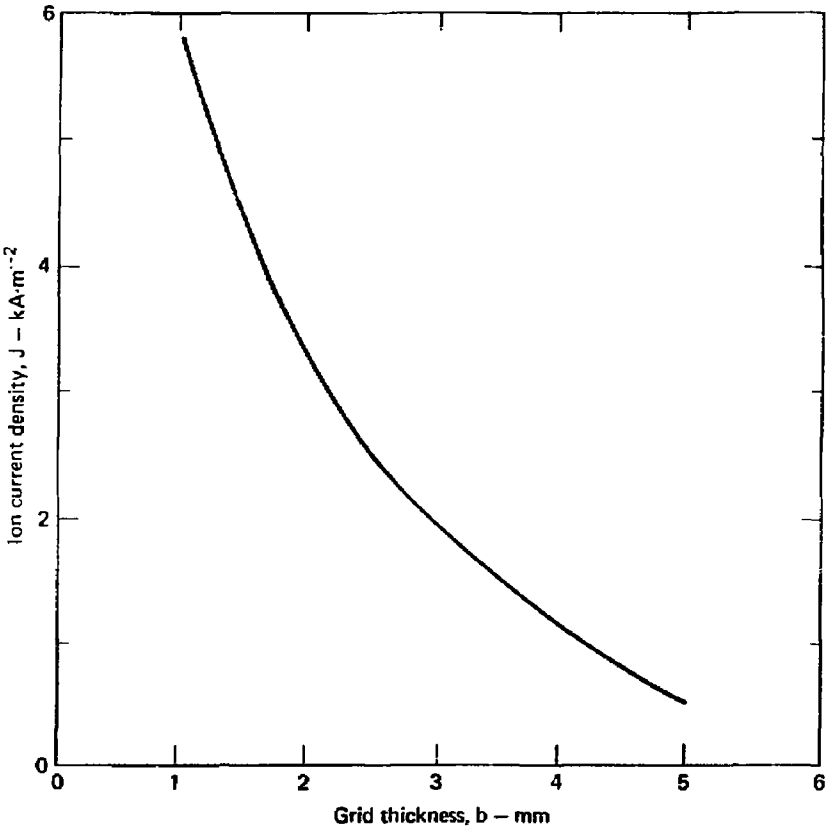


Fig. 7. Extracted ion current density as a function of grid thickness for $E_{av} = 0.75\ MV \cdot m^{-1}$.

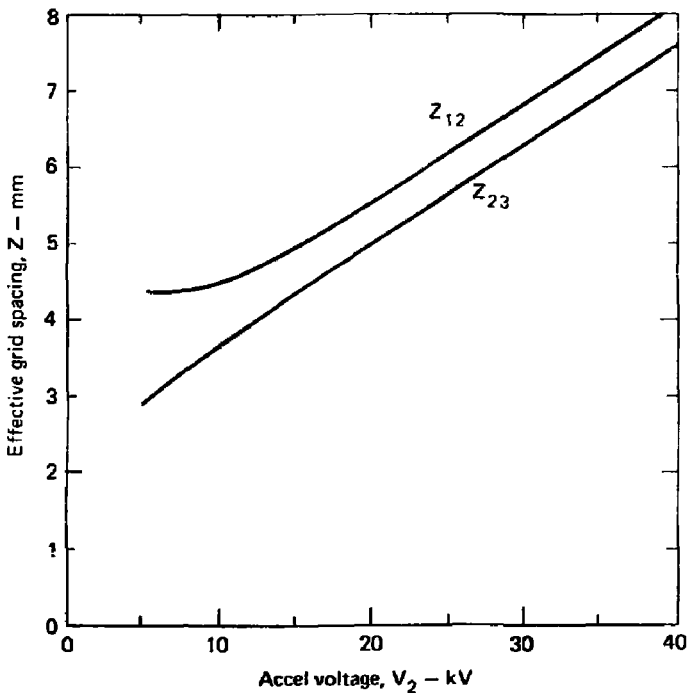


Fig. 8. Variation of spacing in a three-grid extractor as a function of the accel voltage for a grid thickness b = 2.5 mm and an average stress field $E_{av}$ = 0.75 MV•m$^{-1}$.

Electrons released by ionization of the gas do not significantly contribute to grid heating. They tend to follow the path of the positive ion beam back into the ion source, where they do little harm. However, those electrons that are the product of secondary emission caused by ion bombardment of one grid can contribute considerable energy to a neighboring, more positively biased grid. At 15 kV, the secondary emission[2] coefficient for deuterium ions on a clean tungsten surface is about 1. The ion bombardment that initiates the secondary emission tends to sputter any contaminant away and keeps the grid surface clean. Hence, one electron is emitted per incident ion.

Because the grids are designed to operate at a relatively high thermal loading, no allowance need be made for the small contribution of the ion source plasma to grid 1 heating. Even the power radiated from the ion source cathode can be neglected, because it is not significant in a source designed for prolonged, continuous operation.

We estimate grid loading by assuming that all ions, formed between any two grids, accelerate toward the most negative grid in the vicinity. As a consequence, the ions arrive with an average energy equal to half the grid-to-grid potential. In the three-grid extractor, the ions formed between grid 1 and grid 2 bombard grid 2 from the grid 1 side with an average energy equal to $1/2(V_2-V_1)$. Similarly, the other side of grid 2 is bombarded with ions at an average energy of $1/2(V_2-V_3)$.

Let $(F_{10} + F_i)$ be the fraction of the primary ion beam current that is equivalent to the rate at which low-energy ions are formed along the beam path by charge exchange and ionization. Then, the average power density loading of grid 2 from ion bombardment of the grid 1 side of grid 2, is

$$W_{12} = 1/2\ mJ(F_{10} + F_i)_{12}\ (V_2 - V_1)\ ,$$

in which m, the ratio of the spacing between grid rods a to the grid rod width g, is related to the grid transparency $T_g$ by

$$T_g = \frac{m}{1 + m}\ .$$

On the grid 3 side of grid 2,

$$W_{23} = 1/2\ mJ(F_{10} + F_i)_{23}\ (V_2 - V_3)\ .$$

In a short path Z through a background gas density n, the fraction of the beam ions that suffers charge exchange and ionization is

$$(F_{10} + F_I) = n \int_0^Z (\sigma_{10} + \sigma_i)\ dZ\ ,$$

where $\sigma_{10}$ and $\sigma_i$ are the charge-exchange and ionization cross sections, respectively.

Because the cross sections are functions of the incident beam energy, it is convenient to describe the beam path in terms of the beam energy. From Child's law,

$$dZ = 3/4\ (q/J)^{1/2}\ V^{-1/4}\ dV\ .$$

Therefore,

$$(F_{10} + F_i)_{12} = 3/4\ n_{12}\ (q/J)^{1/2} \int_{V_1}^{V_2} (\sigma_{10} + \sigma_i)\ V^{-1/4}\ dV\ ,$$

$$(F_{10} + F_i)_{23} = 3/4\ n_{23}\ (q/J)^{1/2} \int_{V_2}^{V_3} (\sigma_{10} + \sigma_i)\ V^{-1/4}\ dV\ .$$

Values of the integrals[3] are shown in Fig. 9.

The background gas densities $n_{12}$, $n_{23}$ between grids 1 and 2 and grids 2 and 3 are estimated by assuming an equal pressure drop across each of the three grids. As can be seen with the help of Fig. 10, the density between the $N^{th}$ and the $(N + 1)^{th}$ grids is

$$n = \frac{P_s}{KT_G}\left[1 - \frac{N}{N_T}\left(1 - \frac{P_F}{P_s}\right)\right],$$

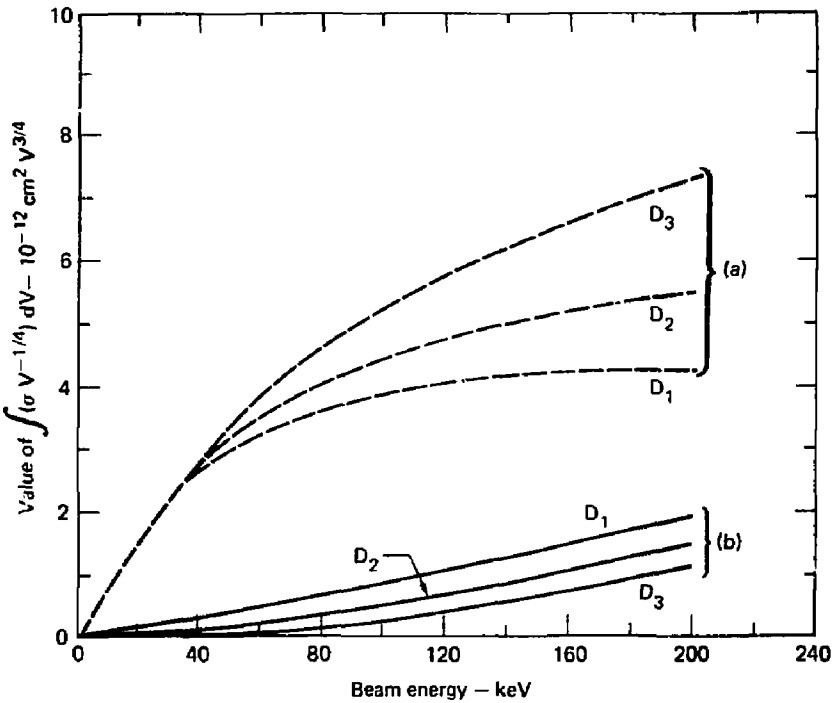


Fig. 9. Cross-section integrals: (a) $\int_0^V \left(\sigma_{10}\, v^{-1/4}\right) dv$ and (b) $\int_0^V \left(\sigma_i v^{-1/4}\right) dv$.

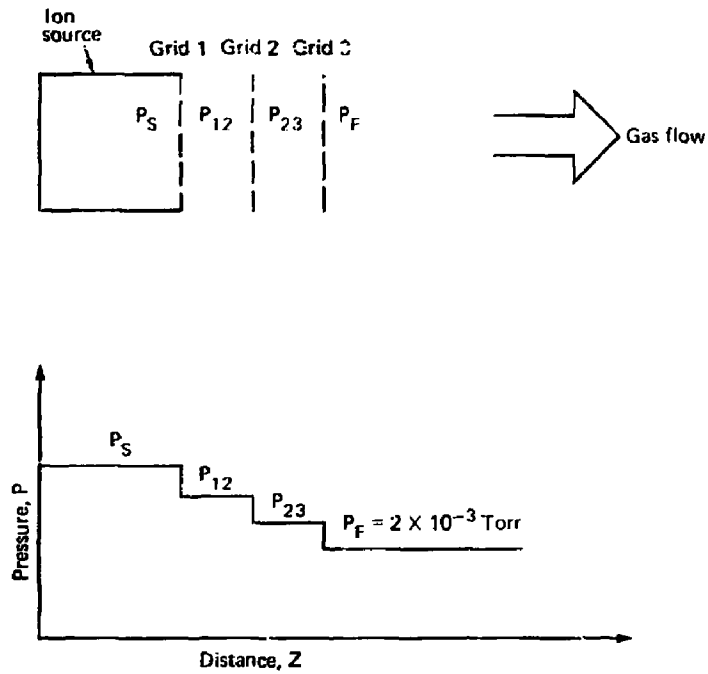


Fig. 10. Approximate pressure profile through the 1-keV extractor.

in which $P_s$ is the pressure of the ion source, $P_F$ is the pressure beyond the last grid, $T_G$ is the background gas temperature, and $N_T$ is the total number of grids in the system.

Over a limited range, the pressure in the ion source is roughly proportional to the extracted ion current density. A deuterium beam of 0.5 $A \cdot cm^{-2}$ has been extracted from a Berkeley-type ion source[4] at a pressure of $10^{-2}$ Torr. Therefore, as an approximation, let

$$P_s = (2 \times 10^{-2}) \quad .$$

In a three-grid system for which $N_T = 3$, $T_G = 1000$ K, and $P_F = 2 \times 10^{-3}$ Torr,

$$n_{12} = (2 \times 10^{14})(0.67\ J + 0.03) \ ,$$
$$n_{23} = (2 \times 10^{14})(0.033\ J + 0.07) \quad .$$

By substituting these values into the previous equations, we can estimate the ion bombardment power densities $W_{12}$, $W_{23}$. These power loading densities are plotted as functions of the accel potential $V_2$ in Fig. 11, along with their sum $W_G$ (the total loading on grid 2). In the above we assume that the grid transparency is 50%, whereby the factor $m = 1$.

In an extractor designed for continuous operation, grid sputtering can be critical. The maximum ion current density bombarding grid 2 is

$$J_B = mJ\ (F_{10} + F_i)_{12} \ .$$

With $V_2$ at 15 kV, this results in $3 \times 10^{-3}$ $A \cdot cm^{-2}$.

The grid sputtering occurs at a rate,

$$S = q_s \left(\frac{M_W}{e\rho}\right) J_B \quad ,$$

in which $M_W$ is the mass of tungsten, $\rho$ is the density of tungsten, and the sputtering of deuterium ions on tungsten results in $q_s = 10^{-3}$ atoms per incident ion.[5] Accordingly, in 6 months the material sputtered away from grid 2 at 15 kV is 0.04 mm; this is not serious.

Favorable ion optics require the separation a between grid rods to be of the order of the effective grid spacing $z_{12}$. To minimize the effect of

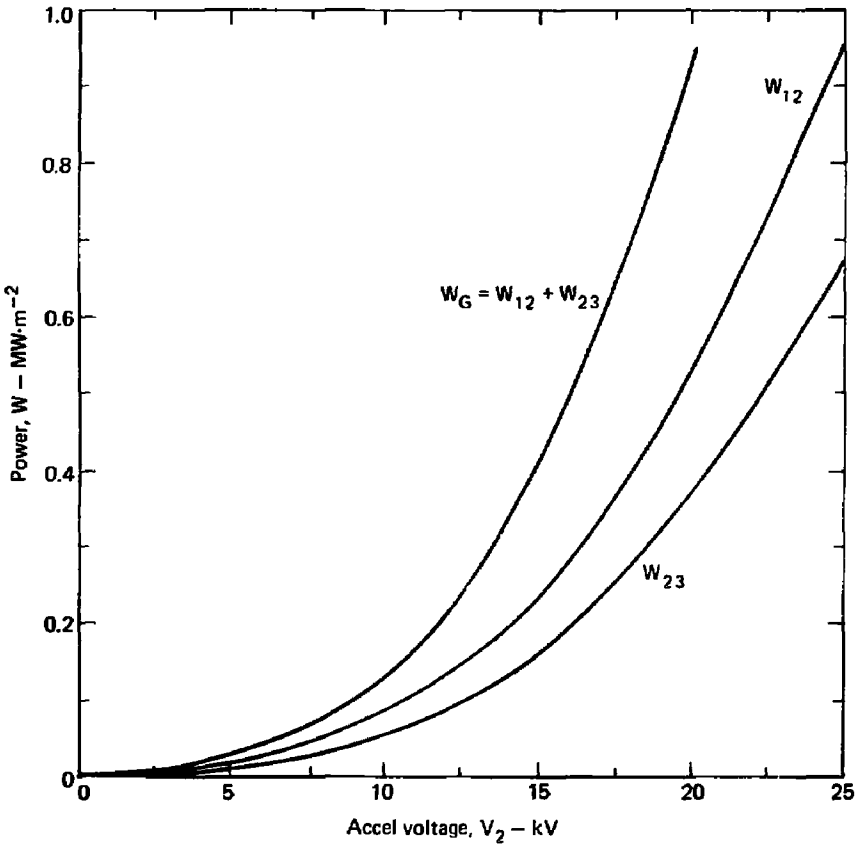


**Fig. 11. Power loading on grid 2.**

the extreme ends of the grid slots,[6] the grid slot length L (twice the length of an individual grid rod) must be at least 10 a. Therefore,

$$a \approx z_{12} \cdot$$
$$a \leq (L/10) \cdot$$

In practice, a is made equal to whichever is the smaller, $z_{12}$ or (L/10).

## HEAT TRANSFER ALONG THE GRID RODS

In the previous section, we determined that the ions formed between grids 1 and 2 bombard grid 2 with a power density $W_{12}$. Similarly, ions originating between grids 2 and 3 bombard the opposite side of grid 2 with a power density $W_{23}$. As a consequence, the heat flow at grid 2 results from the sum of these power densities; i.e.,

$$W_{12} + W_{23} = \varepsilon\sigma \left(2T_2^4 - T_1^4 - T_3^4\right) - 2/3 \text{ kb} \frac{d^2T_2}{dX^2} \cdot$$

In the preceding equation, $\varepsilon\sigma \left(T_2^4 - T_1^4\right)$ is the net radiation per unit area of grid 2 toward grid 1. Likewise, $\varepsilon\sigma \left(T_2^4 - T_3^4\right)$ is the net radiation from grid 2 toward grid 3. Meanwhile, $2/3 \text{ kb } d^2T_2/dX^2$ is the thermal conduction along the grid rod toward the water-cooled frame.

The temperatures of grids 1, 2, and 3 are designated $T_1$, $T_2$, and $T_3$; $\varepsilon$ is the grid emissivity (0.23 for tungsten); $\sigma$ is the Stephan-Boltzman constant ($5.67 \times 10^{-8}$ W•cm$^{-2}$•K$^{-4}$); k is the thermal conductivity (113 W•m$^{-1}$•K$^{-1}$ for tungsten); and b is the thickness of the grid rod.

The factor 2/3 allows for a reduction in cross section resulting from contouring the edges of the grid rods to obtain a preferred ion extraction geometry. Thus, a grid rod of width g and thickness b has a cross-sectional area of about 2/3 gb.

We can write a similar heat flow equation for grid 1, assuming that the secondary emission coefficient at grid 2 is 1 and that all of the electrons arriving at grid 1 come from the grid 1 side of grid 2. Thus, the

current of electrons at grid 1 equals the current of ions bombarding the grid 1 side of grid 2.

The average energy of the ions arriving at grid 2 is 1/2 $(V_2 - V_1)$, while the energy of the electrons arriving at grid 1 is twice that, i.e., $(V_2 - V)$. Hence, the heat flow at grid 1 is

$$2W_{12} = \varepsilon\sigma \left(2T_1^4 - T_2^4\right) - 2/3 \text{ kb} \frac{d^2T_1}{dx^2} \quad ,$$

where the power per unit area conveyed by the electrons is $2 W_{12}$, $\varepsilon\sigma \left(T_1^4 - T_2^4\right)$ is the net radiation per unit area from grid 2, and $\varepsilon\sigma T_1^4$ is the radiation from grid 1 toward the ion source.

From similar reasoning, the heat flow at grid 3 is:

$$2W_{23} = \varepsilon\sigma \left(2T_3^4 - T_2^4\right) - 2/3 \text{ kb} \frac{d^2T_3}{dx^2} \quad .$$

The heat flow equation for grid 2 can be written in a more general form; i.e.,

$$W_G = \varepsilon\sigma \zeta_N T_N^4 - 2/3 \text{ kb} \frac{d^2T_N}{dx^2} \quad ,$$

by defining $\zeta_N$, as

$$\zeta_1 = \left[2 - (T_2/T_1)^4\right] ,$$
$$\zeta_2 = \left[2 - (T_1/T_2)^4 - (T_3/T_2)^4\right] ,$$
$$\zeta_3 = \left[2 - (T_2/T_3)^4\right] ,$$

and by assuming that the temperature ratios do not vary significantly over the grid length.

If the temperatures of grid 1 and grid 3 are such that negligible power is radiated back to grid 2, then $\zeta_2 = 2$. Should grid 1 and grid 3 radiate back 50% of the power radiated away from grid 2, then $\zeta_2 = 1$. Finally, should grid 1 and grid 3 radiate back all of the power radiated

away from grid 2, then $\zeta_2 = 0$. This latter case is the most extreme, for it assumes that all the heat is removed from the grid 2 rods by conduction only.

The heat flow equation can be solved for grid 2 by establishing the coordinate X = 0 at the free end of the grid rod where the temperature $T_M$ is maximum.

Accordingly,

$$X = \left(\frac{5kbT_m}{3W_G}\right)^{1/2} \int_1^T \frac{d\tau}{\left(5 - \alpha\zeta_2 - 5\tau + \alpha\zeta_2\tau^5\right)^{1/2}} ,$$

in which

$$\tau = T/T_M ,$$

$$\alpha = \frac{\epsilon\sigma T_M}{W_G} .$$

For the case of pure conduction, $\zeta_2 = 0$ and

$$X = \left(\frac{4kbT_M}{3W_G}\right)^{1/2} (1 - \tau)^{1/2} .$$

To prevent the grid from getting hot enough to support thermionic emission, let the maximum temperature $T_M = 1700$ K. At this temperature, the emitted electron current density is less than $10^{-4}$ kA·m$^{-2}$. Meanwhile, the temperature at the water-cooled back of the comb is kept at $T_L = 400$ K. Accordingly, the grid rod length (i.e., half the actual grid width) for b = 2.5 mm becomes

$$X_L = \left(\frac{4kb}{3W_G}\right) (T_M - T_L)^{1/2} = 22 W_G^{-1/2} \quad .$$

This relationship is shown in Fig. 12. (Note that the length of the grid rod is inversely proportional to the square root of the power loading of the grid.)

## GRID TEMPERATURE IN AN EXTRACTOR DESIGN

The choice of accel voltage $V_2$ in a three-grid extractor is somewhat arbitrary. Although increased voltages lead to higher extracted ion current densities, too large a voltage can cause voltage stand-off problems. Furthermore, a high current density, which entails a smaller ion source for a given beam current, is not necessarily advantageous. To keep the maximum possible temperature of the grid rods at or below 1700 K, we must reduce the length of the grid rods as the extracted ion current density is increased. Figure 13, which is derived from Figs. 9, 11, and 12, shows how the grid width must be changed for different grid power loadings.

As a compromise, we choose $V_2$ = 15 kV. This results in an extracted ion current density of 2.5 $kA \cdot m^{-2}$, and a grid rod length of 35 mm. In the following discussion, the extractor beam current is taken to be 35 A. Accordingly, the required height of a grid of 50% transparency (m = 1) is 0.4 m. Details of the extractor are shown in Fig. 1; the dimensions are listed in Table 1.

According to Fig. 11, grid 2 at 15 kV must sustain a power loading of 0.4 $MW \cdot m^{-2}$. If that energy were drawn from the grid rods by conduction only, the total power removed from each side of the grid would have to be:

$$P_T = W_G \left(\frac{gX_L H}{a + g}\right) = 2.8 \text{ kW}$$

For this heat to be removed[6] by forced convection, a water channel with an area $A_W$ = 7.5 $mm^2$ is needed. A temperature rise $\Delta T$ of 25°C will entail a water velocity of

$$v = \frac{P_T}{A_W \rho C_p \Delta T} = 3.57 \text{ m} \cdot \text{s}^{-1} \quad ,$$

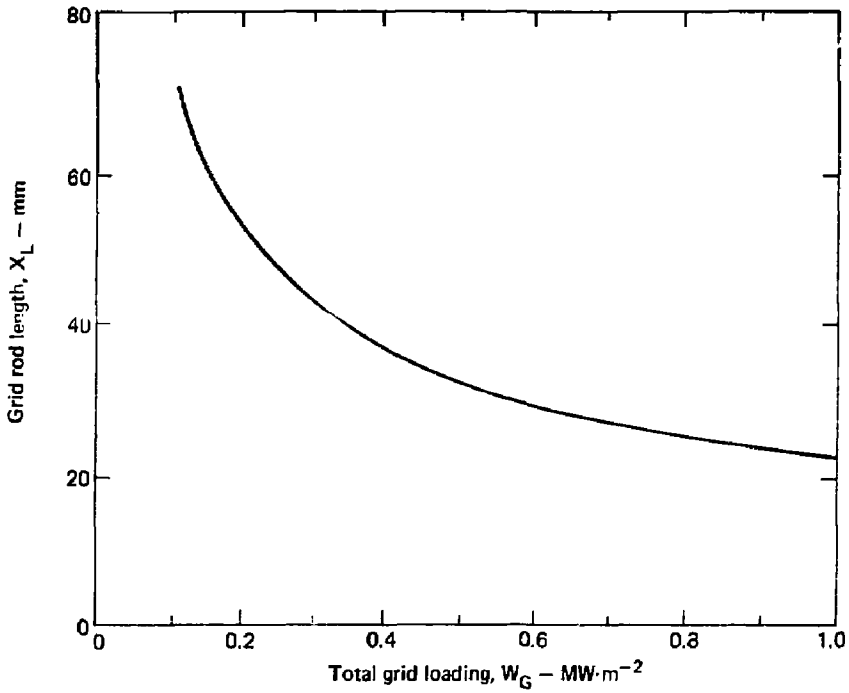


Fig. 12. Allowable length of the grid rod (i.e., half the actual grid width) with a maximum temperature of 1700 K for a grid thickness b = 2.5 mm. We assume thermal conduction but neglect radiation.

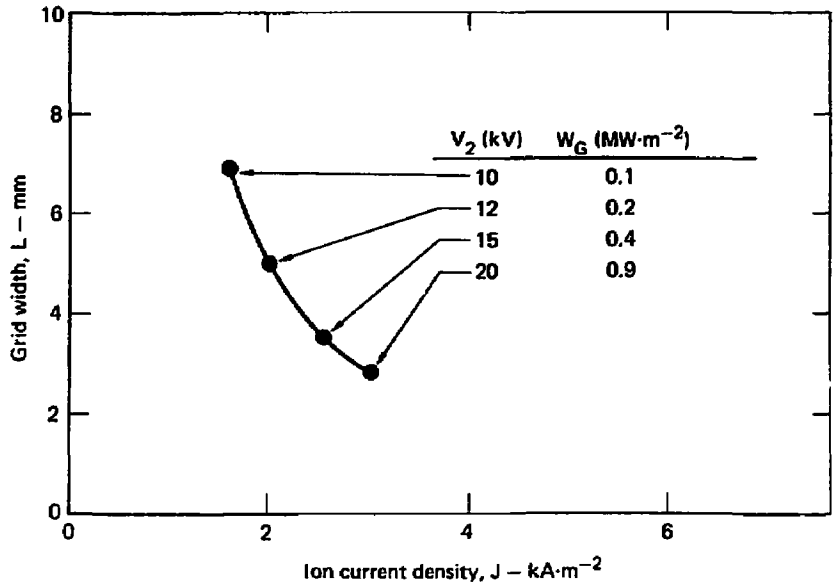


Fig. 13. The grid width required to maintain, by conduction only, a maximum grid temperature $T_M$ = 1700 K as a function of the current density of the extracted ions. Calculations are for a 2.5-mm-thick grid and a maximum field stress of 0.75 MV·m$^{-1}$. Data points show corresponding values of accel voltage $V_2$ and total grid loading $W_G$.

Table 1. 1-keV extractor design.

| Characteristic | Value |
|---|---|
| **Grid potentials:** | |
| Grid 1 | $V_1 = 0$ |
| Grid 2 | $V_2 = 15$ kV |
| Grid 3 | $V_3 = 1$ kV |
| **Grid spacings:** | |
| Grid 1 - Grid 2 | $z_{12} = -5.0$ mm |
| Grid 2 - Grid 3 | $z_{23} = -4.4$ mm |
| **Grid dimensions:** | |
| Rod length | $X_L = 35$ mm |
| Rod width | $g = 50$ mm |
| Slot length | $L = 70$ mm |
| Slot width | $a = 5$ mm |
| Height | $H = 400$ mm |
| Thickness | $b = 2.5$ mm |
| Cooling channels | $X_W = 1.5$ mm |
| | $Y_W = 5$ mm |
| **Extractor performance:** | |
| Extracted ion current | $I^+ = 35$ A |
| Extracted ion current density | $J = 2.5$ kA$\cdot$m$^{-2}$ |
| Rated grid power loading | $W_G = 0.4$ MW$\cdot$m$^{-2}$ |

in which the water density $\rho = 1 \times 10^3$ kg•m$^{-3}$ and the specific heat of water $C_p$ is $4.18 \times 10^3$ J•kg per $^{o}$C.

The pressure drop across the water line is

$$\Delta P = 1/2\ \rho V^2 H\ f/r_e\ ,$$

where the grid height H is 0.4 m, the effective radius is

$$r_e = (A_w/\pi)^{1/2} = 1.5\ \text{mm}\ ,$$

and the friction factor is

$$f = 0.32\ R_e^{-0.25}\ .$$

The Reynolds number can be evaluated from

$$R_e = \frac{2\rho v r_e}{\mu} = 1.07 \times 10^4\ ,$$

where the viscosity of water $\mu$ is approximately $10^{-3}$ kg•m$^{-1}$•s$^{-1}$ at 60$^{o}$C.

Thus, $f = 3.15 \times 10^{-2}$, and the pressure drop is found to be $5.35 \times 10^4$ N•m$^{-2}$.

The temperature rise from the water to the channel wall is

$$\Delta T_{ww} = P_T/(A_c h)\ ,$$

in which $A_c$ represents the surface area of the water channel. For a channel 1.5 × 5 mm,

$$A_c = 2(1.5 + 5.0)\ H\ ,$$

while the heat coefficient h is

$$h = 1/2\ N_\mu\ (k_w/r_e).$$

In the above, the thermal conductivity of water $k_w = 0.65\ W \cdot m^{-1}$ per $^{o}C$, while the Nussult number is

$$N_\mu = 0.023\ R_e^{0.8}\ P_r^{0.4}\ .$$

The Prantl number $P_r = 3$ for water at $60^{o}C$; therefore, the Nussult number $N_\mu = 59.7$, and the heat coefficient $h = 1.29 \times 10^{-2} = MW \cdot m^{-2}$ per $^{o}C$. This results in a temperature rise $\Delta T_{ww} = 42^{o}C$.

With the water-cooling channel located a distance $X_c = 1.5$ mm from the end of the grid rods, the temperature rise from channel wall to rod end is

$$\Delta T_{wR} = \left(\frac{X_c P_T}{bHk}\right) = 37^{o}C\ ,$$

in which $k = 113\ W \cdot m^{-1}$ per $^{o}C$, the thermal conductivity of tungsten.

Thus, the total temperature rise, from the water to the ends of the grid rods, is

$$T_{ww} + T_{wR} = 79^{o}C\ ,$$

while the water temperature rises $25^{o}C$ as it passes through the length of the grid.

The temperature distribution over the grid rods can be calculated for the case where practically all the energy radiated from grid 2 is radiated back, i.e., where there is a negligible radiation loss. By rearranging a previously derived equation, we obtain

$$T = T_M - \left(\frac{3W_G}{4kb}\right) X^2\ ,$$

in which X, the distance along the grid rod, is zero at T = 1700 K. With $T_L = 400$ K on the grid frame, at $X_L = 35$ mm, the temperature distribution is as shown in Fig. 14.

If only 50% of the energy radiated from grid 2 were radiated back, a condition previously discussed would prevail whereby $\zeta_2 = 1$. The

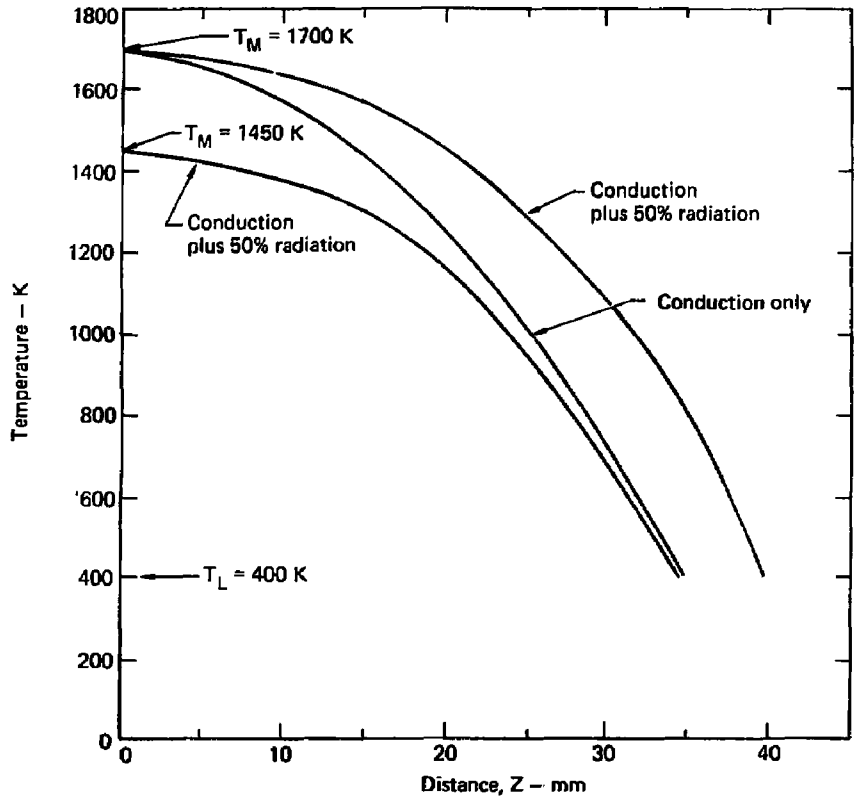


Fig. 14. Temperature variation as a function of the distance along the grid rod measured from the free end. $T_M$ and $T_L$ mark the maximum temperatures and the temperature at the back of the water-cooled comb, respectively.

distance X from the free end of the grid rod to the point where the temperature $T = (\zeta T_M)$ is

$$X = \left(\frac{5kb}{3W_G}\right)^{1/2} \int_1^T \frac{d\tau}{(5 - \alpha - 5\tau + \alpha\tau^5)^{1/2}} \quad .$$

This equation has been solved, and the results are shown in Fig. 14. For a grid rod length of 35 mm, taking radiation into consideration, we find that $T_M$ is only 1450 K. Allowing for radiation, a maximum temperature of 1700 K entails a grid rod length $X_L$ of 40 mm.

From the temperature distribution, the total thermal expansion of a 35 mm-long grid rod was estimated to be 0.23 mm. This requires a gap of about 0.5 mm between cold abutting grid ends to take care of thermal expansion.

## GRID TOLERANCES

Whereas the relationship between the extracted ion current density and the grid-to-grid spacing is described by Child's law, the change in current density that results from a change in spacing can be readily derived; i.e.,

$$\frac{\Delta J}{J} = -2\left(\frac{\Delta Z_{12}}{Z_{12}}\right) \quad .$$

To maintain the current density within $\pm 10\%$ of a specified value, the grid spacing must be held within $\pm 5\%$. Thus, at $Z_{12} = 5.0$ mm, $\Delta Z_{12} = \pm 0.25$ mm.

Variations in grid spacing are the result of several factors, including thermal warping, deflection due to gravity, and electric forces, as well as the variations caused by the normal manufacturing tolerances.

Thermal warping results from one-sided heat loading. As shown in Fig. 15, a power loading $W_G$ can cause a grid rod to bend into a curve that can be approximated by a segment of a circle of radius R. Thus, for a segment enclosed by an angle $\gamma$,

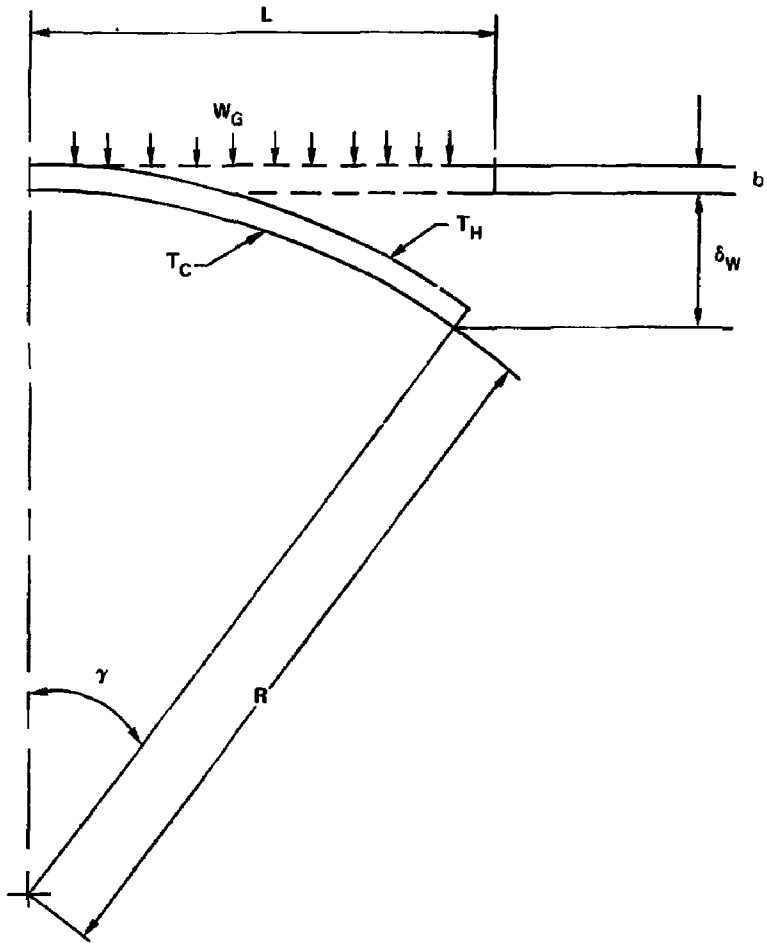


Fig. 15. Warped grid rod. Power loading $W_G$ causes rod deflection $\delta_W$.

$$\gamma = \frac{X_L\ (1 + \alpha_0\ T_C)}{R} = \frac{X_L\ (1 + \alpha_0\ T_H)}{(R + b)} \quad ,$$

where $\alpha_0$ is the thermal coefficient of expansion of the grid (averaging $7 \times 10^{-6}$ for tungsten over the range of temperatures considered), while $T_H$ and $T_C$ are the average temperatures on the hot and cold sides of the grid rod, respectively.

From the above, we find that

$$R = b \left[ \frac{1 + \alpha_0\ T_C}{\alpha_0\ (T_H - T_C)} \right] \quad ,$$

and

$$\gamma = \alpha_0\ (X_L/b)\,(T_H - T_C) \quad .$$

The grid rod deflection is found to be

$$\delta_W = 2\ R\ \sin^2\ (\gamma/2) \quad ,$$

which with $\gamma$ small is approximately

$$\delta_W = 1/2\ R\gamma^2 \quad .$$

Therefore,

$$\delta_W = \frac{\alpha_0 X_L^{\ 2}}{2b}\ (T_H - T_C) \quad .$$

Because most of the incident energy is conducted along the grid rod toward the grid frame, little is conducted across it. Hence,

$$W_G > k\left(\frac{T_H - T_C}{b}\right),$$

and

$$\delta_W < \frac{\alpha_0 X_L^2 W_G}{2k} \quad .$$

We previously determined that

$$W_G X_L^2 = \frac{4kb}{3} (T_M - T_L) ;$$

hence, the deflection is

$$\delta_W < \frac{2\ \alpha_0 b}{3} \ (T_M - T_L) = 0.015 \text{ mm} ,$$

and thermal warping is of little significance.

The grid rods are cantilevered over the face of the ion source. Therefore, they are subject to deflection caused by the force of the electric field between adjacent grids as well as by the force of gravity.

If $\psi$ were the electric energy stored between grids, the force between the grids would be

$$F_E = \frac{d\psi}{dz} ,$$

where

$$\psi = 1/2\ C \cdot V^2 ,$$

and the capacitance between grids is

$$C = \frac{\epsilon_0 A_G}{Z} \quad .$$

Accordingly, the electric force per unit grid area is

$$F_E/A_G = \epsilon_0/2 \ (V/Z)^2 = \epsilon_0 E_{av}^2/2 \ .$$

For a grid mounted in such a position that gravity will enhance the force on the grids, the contribution gravity is

$$F_G/A_G = \rho b \ ,$$

in which the density of the grid material (tungsten) is $\rho = 19.3 \times 10^3$ $kg \cdot m^{-3}$.

The deflection of a cantilevered bar is

$$\delta_b = \frac{\omega_T X_L^4}{8EI} \ ,$$

where the force per unit length is

$$\omega_T = g\left[\epsilon_0 E_{av}^2/2 + \rho b\right] \ .$$

Young's modulus for tungsten is $\bar{E} = 35 \times 10^{11}$ $kg \cdot m^{-3}$, and the moment of inertia is

$$I = \frac{gb^3}{12} \ .$$

If we substitute the grid dimensions from Table 1, we find that the grid rod deflection is $1.4 \times 10^{-6}$ mm, a negligible value.

The deflection of the entire grid frame can be estimated by considering a bar of length H, rigidly held on both ends, see Fig. 16. For this case, the deflection is

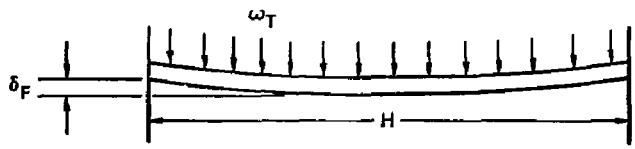


Fig. 16. Deflection of the grid frame under load. Force per unit area $\omega_T$ causes deflection $\delta_F$.

$$\delta_F = \frac{\omega_T H^4}{384\ EI} \quad ,$$

in which the force per unit length $\omega_T$ is as before, and the moment of inertia for a grid frame of width h = 20 mm is

$$I = \frac{hb^3}{12} \quad .$$

Thus, because

$$\delta_F = 0.026 \text{ mm},$$

this deflection is also not of major significance.

As a result, almost the full tolerance $\pm\Delta z_{12}$ that is permissible to hold the extracted current density to within $\pm$10% of the desired value becomes available for variations in parts and assembly.

Grid alignment, another important factor in the construction of the ion extractor, can be evaluated in terms of the angular displacement $\Delta\theta$ of a single beamlet passing through a series of grid rods. The grids are assumed to be parallel and equally spaced. However, grid 2 is displaced by a distance $\Delta y$, as shown in Fig. 17.

An analogy to light optics shows that

$$\Delta\theta = (\Delta y/f) \ ,$$

where f is the focal length of the lens.

For an ion beam, the focal length of a slot-type aperture is approximately[7]

$$f = \frac{2(V_2 - V_1)}{(E_{12} - E_{23})} \quad ,$$

where $E_{12}$ and $E_{23}$ are the electric fields on the grid 1 side and the grid 3 side of grid 2, respectively. From Child's law,

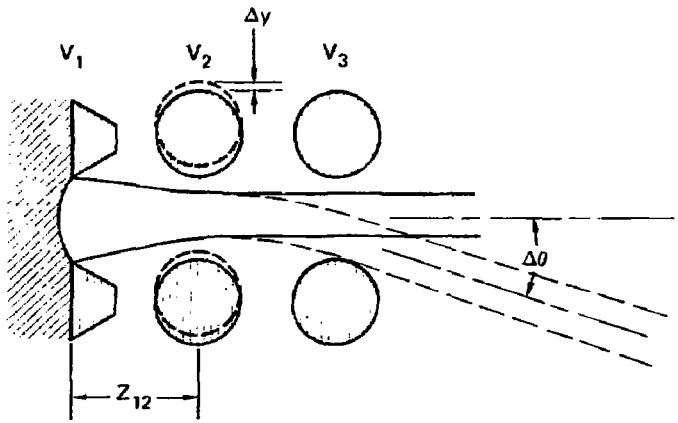


Fig. 17. Effect of an offset grid rod on an ion beamlet. A grid displaced by $\Delta y$ causes an angular displacement $\Delta\theta$.

$$E_{12} = 4/3\ (V_2/z_{12}) \quad ,$$

and

$$E_{12} \quad -E_{23} \ .$$

Therefore,

$$\Delta\theta = 4/3\ (\Delta y/z_{12}) \ .$$

The current density distribution across a beamlet is approximately Gaussian, such that

$$J_{(\ell,y)} = A_0 \exp\left[-(y/y_e)^2\right] ,$$

in which $A_0$ is a function of the distance $\ell$ from the virtual source of the beam to the plane in which the current density is measured, and $y_e$ is that displacement from the beamlet axis at which the current density is 1/e times its peak value.

If grid 2 were displaced by $\Delta y$, the beam axis at $\ell$ would shift by

$$s = \ell\ \Delta\theta = 4/3\ \ell\ (\Delta y/z_{12}) \ ,$$

and the current density distribution would become

$$J_{(\ell,y)} = A_0 \exp\left[-\left(\frac{y - s}{y_e}\right)^2\right] .$$

For a small displacement off-axis at $y = y_e$, the fractional change in current density is

$$\frac{\Delta J}{J} = 1 - \exp\left[-\left(\frac{2s}{y_e}\right)\right] = 2s/y_e \ .$$

If $\theta_T$ is defined as that angle in the beamlet at which the current density is 1/e times its peak value, then

$$y_e = \ell\theta_T ,$$

and from the above,

$$\Delta y = \frac{3\,\theta_T z_{12}}{8}\left(\frac{\Delta J}{J}\right) .$$

In a 20-keV deuterium beam[4] extracted from a Berkeley-type ion source, the current density falls to 1/e times its peak value at an angle of $1.5^{\circ}$, perpendicular to the grid rods. Because the beam angle varies inversely with the square root of the beam energy, $\theta_T = 0.17$ radians at 1 keV.

Thus, we find that a 10% change in the current density at the off-axis 1/e point entails a grid displacement of $\Delta y = 0.032$ mm.

The effect of a random misalignment of all of the grid rods is very different from that resulting from a net displacement of the grid to one side. The random displacement causes the beam to spread out and form a somewhat broader focus, whereas a net displacement deflects the beam. If the grid rods are located within the limit established above, there will be little problem in either case.

## CONCLUSION

A critical design feature in a continuously operated ion source is grid cooling. Whereas the grid rods can be cooled by heat pipes or possibly by forced convection using liquid metals, water, or pressurized gas, we present a simpler solution. Using solid-tungsten grid rods brazed to the grid frame and allowed to expand toward the grid center, 0.4 $MW \cdot m^{-2}$ can be handled with a total grid width of about 70 mm. Calculations show that thermal distortion is minimal. The only undesirable feature is the grid rod expansion gap at the grid center. We estimate that the grid gap is 0.5 mm when the grid is cold, but that it will be only 0.05 mm when the grid runs hot. Thus, a relatively simple grid structure can be used to form an extractor of a continuous 1-keV positive ion beam.

## REFERENCES


1. J. H. Fink and C. E. McDowell, "Ionization, Charge Exchange and Secondary Electron Emission in the Extractor of an LBL/LLL Neutral Beam Source," in *Proc. Sixth Symp. Engineering Problems of Fusion Research, San Diego, CA* (IEEE, 1975), p. 161.
2. N. N. Petrov, "Secondary Emission from Metals Under the Influence of Positive Ions," *Izv. Akad. Nauk SSSR Acad. Sci. USSR* [*Bull. Acad. Sci. USSR*] 26 1350 (1962).
3. J. H. Fink and D. J. Bender, *A Proposed 268-MW Neutral-Beam Injector for the Hybrid Mirror Reference Reactor*, Lawrence Livermore Laboratory, Rept. UCRL-80577 (1978).
4. K. W. Ehlers, W. R. Baker, K. H. Berkner, W. S. Cooper, W. B. Kunkel, R. V. Pyle, and J. W. Stearns, "Large Area Plasma Sources," in *Proc. Second Symp. Ion Sources and Formation of Ion Beams, Berkeley, CA* (APS, 1974), I-5.
5. C. R. Finfgeld, *Proton Sputtering*, AEC Rept. ORO-3557-15 (undated).
6. W. M. Kays, *Convective Heat and Mass Transfer* (McGraw-Hill, New York, 1966).
7. J. R. Copeland and T. S. Green, "Ion Beam Deflection in Extraction Electrodes," *Nucl. Instrum. Methods* 125, 197 (1975).


CKM